Orbital Dependent Electronic Masses in Ce Heavy Fermion Materials studied via Gutzwiller Density Functional Theory

Ruanchen Dong,[1] Xiangang Wan,[2] Xi Dai,[3] and Sergey Y. Savrasov[1]

[1]*Department of Physics, University of California Davis, Davis, California 95616, USA*
[2]*National Laboratory of Solid State Microstructures and Department of Physics, Nanjing University, Nanjing 210093, China*
[3]*Beijing National Laboratory for Condensed Matter Physics and Institute of Physics, Chinese Academy of Sciences, Beijing 100190, China*

(Dated: March 14, 2014)

A series of Cerium based heavy fermion materials is studied using a combination of local density functional theory and many–body Gutzwiller approximation. Computed orbial dependent electronic mass enhancements parameters are compared with available data extracted from measured values of Sommerfeld coefficient. The Gutzwiller density functional theory is shown to remarkably follow the trends across a variety of Ce compounds, and to give important insights on orbital selective mass renormalizations that allow better understanding of wide spread of data.

PACS numbers:

arXiv:1401.5912v3 [cond-mat.str-el] 12 Mar 2014

I. INTRODUCTION

Heavy fermion materials pose one of the greatest challenges in condensed matter physics. Their low–temperature linear specific heat coefficient can be up to 1000 times larger than the value expected from the free–electron theory; their magnetic moments can be screened by the Kondo effect and their electrical resistivity is frequently divergent but sometimes superconductivity can emerge at low temperatures[1].

Theoretical calculations based on density functional theory (DFT) in its popular Local Density Approximation (LDA)[2] fail to reproduce strongly renormalized electronic masses in heavy fermion materials due to improper treatment of many–body correlation effects. Consider, for example, a well–known class Cerium class of heavy fermion materials, such as two famous phases (α and γ) of Cerium itself[3–5], so called Ce–115s systems: $CeXIn_5$ (X=Co,Rh,Ir)[6–8] and numerous Ce–122 compounds[9–21]: CeX_2Si_2 (X=Mn,Fe,Co,Ni,Cu,Ru,Rh,Pd,Ag). A Table 1 gives evaluated via LDA densities of states specific heat coefficients γ for these materials as compared to experiments, where in many cases a factor of 2–20 error exists in underestimating γ while in some cases, such, e.g., as $CeCo_2Si_2$, an overestimation occurs. It is the purpose of this work to show that a better treatment of electronic correlations via a recently introduced Gutzwiller Density Functional Theory[22–25] can correct most of these errors and uncover which exactly orbitals become heavy as is also illustrated in Table I.

The physics of the electronic mass enhancement is controlled by a low frequency behavior of the local electronic self–energy which can be encoded in a simple Teilor like form

$$\Sigma_\alpha(\omega) = \Sigma_\alpha(0) + (z_\alpha^{-1} - 1)\omega + ... \qquad (1)$$

where we assume, for simplicity, the existence of some crystal field representation $|\alpha\rangle$ that diagonalizes the self–energy matrix in a spin–orbital space of the localized f electrons. This expression suggests two main effects that may occur when correlations are brought into consideration on top of a band theory such as LDA: first the crystal field correction to a local f–electron level is controlled by $\Sigma_\alpha(0)$ and, second, the actual band narrowing is controlled by a quasiparticle residue parameter z_α. Both effects would affect our comparisons of γ in Table 1.

Recently, advanced many body approaches based on combinations of Density Functional and Dynamical Mean Field Theory (DMFT) have been implemented[26] to study heavy fermion systems[27,28] where self–consistent solutions of either Anderson or Kondo impurity problems have been done using most accurate Continues Time Quantum Monte Carlo method[29,30]. While DMFT deals with full frequency dependent self–energy and is a lot more computationally demanding than traditional LDA, it taught us an important lesson on the so called orbital selectivity in the Mott transition problem, i.e. when crystal field dependent self–energies can reduce effective degeneracy of the impurity. This affects the proximity of the quasiparticle residue z to become equal zero when the ratio between Hubbard U and bandwidth W changes.

A recently introduced Gutzwiller Density Functional Theory (GDFT) and the so called LDA+G method[22–25] is a simplified variational approach that relies on the Gutzwiller approximation initially introduced to study itinerant ferromagnetism of the one–band Hubbard model[31], and later extended to multi–band systems[32,33]. In this method, the atomic configurations of correlated orbitals are treated by adjusting their weights using a variational procedure. This leads to renormalized energy bands and mass enhancements for the electrons. The approximation was extensively studied in the limit of infinite dimensions[34,35], and was shown to be equivalent to a slave–boson mean–field theory[36] for both single–band and multiband models[37–39]. In LDA+G, the Gutzwiller type trial wave function $\hat{P}|0\rangle$ is adopted with $|0\rangle$ and $\hat{P}$ being the LDA ground state and the Gutzwiller projector respectively. After further applica-

tion of the Gutzwiller approximation, an effective Hamiltonian describing the dynamics of quasiparticles was obtained as $H_{eff} = \hat{P} H_{LDA} \hat{P}$, which contains two important features discussed above: the modification of the crystal/spin–orbital fields and the quasiparticle weight z_α. Thus, the method exactly casts the effect encoded into the low–frequency behavior of $\Sigma(\omega)$, Eq. (1).

The benchmark of the LDA+G scheme was demonstrated in Ref. 22. For a non–magnetic correlated metal $SrVO_3$, it produced narrower bands and larger effective masses than those found in standard LDA. Also the method was able to get a photoemission peak missed in the LDA calculation. These improvements are very close to the experimental results. Later, in Ref. 40 a complex phase diagram of Na_xCoO_3 was correctly reproduced. Recently, this method has been successfully applied to FeAs–based superconductors[25,41] and to Ce metal[42,43].

In this work we address the physics of Cerium heavy fermion materials via the use of the LDA+G approach. A great spread in the extracted values of mass enhancements data shown in Table I together with some unphysical values of $z > 1$ prompts us that in many classes of real compounds both the orbital selectivity encoded via the shifts $\Sigma_\alpha(0)$ on top of the LDA as well as the quasiparticle residues play an important role and have to be treated on the same footing. It therefore represents a stringiest test of a many body electronic structure method such as LDA+G to heavy fermion materials. In particular, in its recent application to elemental Cerium[43], it has been shown that the spin–orbital splitting of the f–level is renormalized by correlations and pushes energies of the J=7/2 manifold up relative to J=5/2 states. This resulted in lowering the degeneracy from 14 to 6 and in a greater mass enhancement of J=5/2 manifold as compared to a non–spin orbit coupled calculation.

The paper is organized as follows. In Sec. II, the LDA+G method is described. The results for several typical families of heavy fermion materials are presented in Sec. III. Finally, Sec. IV is the conclusion.

II. THE LDA+G METHOD

The Gutzwiller Density Functional Theory and the LDA+G approximation have been described previously[22–25]. Here we merely summarize the equations of the method that we implement using a linear muffin–tin orbital formalism that includes both the full potential terms and relatvistic spin–orbit coupling operator variationally[44] .

A. Gutzwiller Approximation

We first illustrate the method using a general multi–orbital Hubbard model. The Hamiltonian is:

$$H = H_0 + H_{int} = \sum_{ij,\alpha\beta} t_{ij}^{\alpha\beta} c_{i\alpha}^\dagger c_{j\beta} + \sum_i \sum_{\alpha\neq\beta} U_i^{\alpha\beta} \hat{n}_{i\alpha} \hat{n}_{i\beta} \tag{2}$$

where $\alpha = 1, \ldots, 2N$ is the spin–orbital index of the localized orbital, N is the number of orbitals, e.g. 7 for the f–orbital. The first term is a tight–binding Hamiltonian which can be extracted from the LDA calculation. The second term is the on–site interaction which has been restricted to the density–density interaction.

In the atomic limit, for the localized orbital there are $2N$ different states which can be either occupied or empty. Therefore there is total 2^{2N} configurations $|\Gamma\rangle$. All these configurations form a complete basis and the density–density interaction is diagonal in this configuration space. It is obvious that these configurations should not be equally weighted. In the Gutzwiller method, we adjust the weight of each configuration. Therefore it is convenient to construct projection operators that project onto a specific configuration Γ at site i:

$$\hat{m}_{i\Gamma} = |i\Gamma\rangle\langle i\Gamma| \tag{3}$$

When the interaction term is absent, the ground state is the Hatree uncorrelated wave function (HWF) $|\Psi_0\rangle$ which is a Slater determinant of the single–particle states. When the interaction is switched on, this wave function is no longer a good approximation. In the Gutzwiller method, we project the wave function to a Gutzwiller wave function (GWF) $|\Psi_G\rangle$ by adjusting the weight of each configuration through variational parameters $\lambda_{i\Gamma}$ ($0 \leqslant \lambda_{i\Gamma} \leqslant 1$):

$$|\Psi_G\rangle = \hat{\mathcal{P}}|\Psi_0\rangle = \prod_i \hat{P}_i |\Psi_0\rangle \tag{4}$$

where

$$\hat{P}_i = \sum_\Gamma \lambda_{i\Gamma} \hat{m}_{i\Gamma} \tag{5}$$

Notice that when all $\lambda_{i\Gamma} = 1$, the GWF is going back to HWF. At the same time, setting $\lambda_{i\Gamma} = 0$ removes configuration Γ at site i. Therefore, perfectly localized atomic state of site i is described by all $\lambda_{i\Gamma} = 0$ except for one, and in this way, the Gutzwiller wave function captures both the itinerant and localized behavior of the system.

It is a difficult task to evaluate GWF. However, within the Gutzwiller method, we can map any operator $\hat{O}$ acting on the GWF to a corresponding effective $\hat{A}^G$ which acts on the HWF:

$$\langle\Psi_G|\hat{A}|\Psi_G\rangle = \langle\Psi_0|\hat{\mathcal{P}}^\dagger \hat{A} \hat{\mathcal{P}}|\Psi_0\rangle = \langle\Psi_0|\hat{A}^G|\Psi_0\rangle \tag{6}$$

where

$$\hat{A}^G = \hat{\mathcal{P}}^\dagger \hat{A} \hat{\mathcal{P}} \tag{7}$$

TABLE I: Comparison between calculated using LDA density of states and experimentally extracted specific heat coefficients γ and the extracted quasiparticle residues $z_{\rm exp} = \gamma_{LDA}/\gamma_{\rm exp}$ for a number of Cerium based heavy fermion compounds considered in this work. The last columns show the predictions of γ and z using the LDA+G method with the values of U=4 and 5 eV as well as the reference to a specific orbital degeneracy of the $j = 5/2$ manifold that exibits strongest enhancement.

	$N_{LDA}(0)$ St./(Ry·cell)	γ_{LDA} mJ/(mol K^2)	γ_{exp} mJ/(mol K^2)	Ref. to γ_{exp}	$z_{\rm exp}$	γ_{LDA+G} (U=4 eV)	γ_{LDA+G} (U=5 eV)	z_{LDA+G} (U=4 eV)	z_{LDA+G} (U=5 eV)	Orbital $j = 5/2$
α-Ce	36	6.2	13	3	0.48			0.55	0.33	Γ_7,Γ_8
γ-Ce	49	8.5						0.14	0.11	Γ_7,Γ_8
115s:										
$CeCoIn_5$	150	26.0	290	6	0.09	70	104	0.20	0.13	Γ_6,$2\times\Gamma_7$
$CeRhIn_5$	156	27.2	420	7	0.065	75	120	0.19	0.12	Γ_6,$2\times\Gamma_7$
$CeIrIn_5$	165	28.6	720	8	0.04	79	210	0.14	0.07	Γ_6,$2\times\Gamma_7$
122s:										
$CeMn_2Si_2$	184	31.9	47	9	0.68	52	84	0.51	0.43	Γ_6,$2\times\Gamma_7$
$CeFe_2Si_2$	85	14.7	22	10	0.67	21	24	0.53	0.47	Γ_6,$2\times\Gamma_7$
$CeCo_2Si_2$	110	19.0	10	11	1.9?	35	43	0.47	0.36	Γ_6,$2\times\Gamma_7$
$CeNi_2Si_2$	115	19.9	33	12	0.60	27	29	0.47	0.43	Γ_6,$2\times\Gamma_7$
$CeCu_2Si_2$	64	11.1	1000	13–15	0.01	430	∞	0.10	0	Γ_6
$CeRu_2Si_2$	103	17.8	350	16–18	0.05	70	190	0.33	0.13	$2\times\Gamma_7$
$CeRh_2Si_2$	106	18.3	130	19	0.14	35	120	0.36	0.14	$2\times\Gamma_7$
$CePd_2Si_2$	100	17.3	65-110	20,21	0.15-0.26	170	∞	0.045	0	Γ_7
$CeAg_2Si_2$	205	35.5				140	430	0.10	0.06	Γ_6

Specifically, when the operator $\hat{A}$ is a single–particle operator, e.g. $\hat{A} = \sum_{ij,\alpha\beta} A_{ij}^{\alpha\beta} c_{i\alpha}^\dagger c_{j\beta}$ where $A_{ij}^{\alpha\beta} = \langle i\alpha|\hat{A}|j\beta\rangle$, the Gutzwiller effective operator can be written as:

$$\hat{A}^G = \sum_{ij,\alpha\beta} \sqrt{z_{i\alpha}} A_{ij}^{\alpha\beta} \sqrt{z_{j\beta}} c_{i\alpha}^\dagger c_{j\beta} + \sum_{i,\alpha} A_{ii}^{\alpha\alpha}(1 - z_{i\alpha}) c_{i\alpha}^\dagger c_{i\alpha} \tag{8}$$

where $z_{i\sigma}$ are the orbital–dependent quasiparticle residues: $0 \leqslant z_{i\alpha} \leqslant 1$. These are determined by the configuration weights:

$$z_{i\alpha} = \sum_{\Gamma\Gamma'} \frac{\sqrt{m_{i\Gamma} m_{i\Gamma'}} |\langle i\Gamma'|c_{i\alpha}^\dagger|i\Gamma\rangle|}{\sqrt{n_{i\alpha}(1 - n_{i\alpha})}} \tag{9}$$

where $m_{i\Gamma} = \langle\Psi_G|\hat{m}_{i\Gamma}|\Psi_G\rangle$ and $n_{i\alpha}$ are the occupation numbers for the orbitals.

B. Combination with LDA

Similar to the idea of the LDA+U or LDA+DMFT methods, we add the interaction term on top of the LDA calculation. The Hamiltonian is given by:

$$H = H_{LDA} + H_{int} - H_{DC} \tag{10}$$

where $H_{\rm LDA}$ is the LDA Hamiltonian, which casts the same form as H_0 in Eq.(2), $H_{\rm int}$ is the on–site interaction term for the set of correlated orbitals, such as f–orbitals of heavy–fermion materials considered in this work. Since the LDA calculation has already included the Coulomb interaction in some averaged level, we need to subtract the double–counting term H_{DC} from LDA. Various forms of H_{DC} will be discussed later.

The Kohn–Sham approach uses a non–interacting system as a reference which keeps the same density as the interacting one. However, now our ground state is the GWF instead of the HWF. Therefore, we need to transform the Hamiltonian into the effective one in the $|\Psi_0\rangle$ basis. Since the Hamiltonian H_{LDA} is a single–particle operator, following Ref. 24 we obtain

$$\begin{aligned} H_{LDA}^G \;=\; & \langle\Psi_G|H_{LDA}|\Psi_G\rangle = \\ & \left(\sum_{\alpha i} \sqrt{z_\alpha}|\phi_{\alpha i}\rangle\langle\phi_{\alpha i}| + 1 - \sum_{\alpha i}|\phi_{\alpha i}\rangle\langle\phi_{\alpha i}|\right) H_{LDA} \left(\sum_{\beta j} \sqrt{z_\beta}|\phi_{\beta j}\rangle\langle\phi_{\beta j}| + 1 - \sum_{\beta j}|\phi_{\beta j}\rangle\langle\phi_{\beta j}|\right) + \\ & \sum_{\alpha i}(1 - z_\alpha)|\phi_{\alpha i}\rangle\langle\phi_{\alpha i}|H_{LDA}|\phi_{\alpha i}\rangle\langle\phi_{\alpha i}| \end{aligned}$$

where $|\phi_{\alpha i}\rangle$represents a complete basis set of the correlated orbitals, and where we omit site index i from the quasiparticle residues $z_a$due to lattice periodicity.

The interaction term acting on the GWF produces:

$$H^G_{int} = \langle \Psi_G | H_{int} | \Psi_G \rangle = \sum_{i\Gamma} E_\Gamma m_\Gamma \tag{11}$$

The expectation value of the total Hamiltonian gives us the total energy as a functional of the density ρ and confugurational weights m_Γ:

$$E(\rho, \{m_\Gamma\}) = \langle \Psi_0 | H^G_{LDA} | \Psi_0 \rangle + \sum_\Gamma E_\Gamma m_\Gamma - E_{DC} \tag{12}$$

A minimization similar to LDA is now performed. Representing density in terms of the Kohn–Sham states, produces the equations for the quasiparticles:

$$\frac{\partial E(\rho, \{m_\Gamma\})}{\partial \langle \psi_{nk}} = \left(H^G_{LDA} + \sum_\alpha \left[\frac{\partial E}{\partial z_\alpha} \frac{\partial z_\alpha}{\partial n_\alpha} - \frac{\partial E_{DC}}{\partial n_\alpha} \right] |\phi_\alpha\rangle\langle\phi_\alpha| \right) |\psi_{nk}\rangle = \epsilon_{nk} |\psi_{nk}\rangle \tag{13}$$

$$\frac{\partial E(\rho)}{\partial m_\Gamma} = \sum_\alpha \frac{\partial E}{\partial z_\alpha} \frac{\partial z_\alpha}{\partial m_\Gamma} + E_\Gamma = 0 \tag{14}$$

Recalling the self–energy linear expansion, Eq.(1), we see from Eq.(13) that the effective Hamiltonian to be diagonalized casts the following form

$$H^G = H^G_{LDA} + \sum_\alpha (\Sigma_\alpha(0) - V_{DC,\alpha}) z_\alpha |\phi_\alpha\rangle\langle\phi_\alpha| \tag{15}$$

where $\Sigma_\alpha(0)$ and $V_{DC,\alpha}$ are directily associated with various total energy derivatives appeared in (13).

C. Gutzwiller Projected Hamiltonian

It is convinient to represent all matrices in the space of the Bloch eigenvalues $\epsilon_{\mathbf{k}j}$ and wave functions $|\mathbf{k}j\rangle$ that are obtained from the LDA calculation. The Gutzwiller hamiltonian to be diagonalized is given by

$$\begin{aligned} \langle \mathbf{k}j' | H^G | \mathbf{k}j \rangle \;=\; & \sum_{j''} \epsilon_{\mathbf{k}''j''} \left(\sum_\alpha \sqrt{z_\alpha} \langle \mathbf{k}j' | \phi_\alpha \rangle\langle \phi_\alpha | \mathbf{k}j'' \rangle + \delta_{j'j''} - \sum_\alpha \langle \mathbf{k}j' | \phi_\alpha \rangle\langle \phi_\alpha | \mathbf{k}j'' \rangle \right) \times \\ & \left(\sum_\beta \sqrt{z_b} \langle \mathbf{k}j'' | \phi_\beta \rangle\langle \phi_\beta | \mathbf{k}j \rangle + \delta_{j''j} - \sum_\beta \langle \mathbf{k}j'' | \phi_\beta \rangle\langle \phi_\beta | \mathbf{k}j \rangle \right) + \sum_\alpha (1 - z_\alpha) \langle \mathbf{k}j' | \phi_\alpha \rangle \epsilon_\alpha \langle \phi_\alpha | \mathbf{k}j \rangle + \\ & \sum_\alpha \left(\Sigma_\alpha(0) - V_{DC,\alpha} \right) z_\alpha \langle \mathbf{k}j' | \phi_\alpha \rangle\langle \phi_\alpha | \mathbf{k}j \rangle \end{aligned} \tag{16}$$

where a subset of correlated orbitals $|\phi_\alpha\rangle$ is introduced. Their levels are given by

$$\epsilon_\alpha = \sum_{\mathbf{k}''j''} \epsilon_{\mathbf{k}''j''} \langle \phi_\alpha | \mathbf{k}''j'' \rangle\langle \mathbf{k}''j'' | \phi_\alpha \rangle \tag{17}$$

The quasiparticle residues z_α and the level shifts $\Sigma_\alpha(0)$ are obtained using the Gutzwiller procedure[24]. The double counting potential $V_{DC,a}$ corrects for the fact that the LDA already accounts for some of the correlation effects in a mean field manner. The eigenvalue problem

$$\sum_j (\langle \mathbf{k}j' | H^G | \mathbf{k}j \rangle - \delta_{j'j} E_{\mathbf{k}n}) B^{\mathbf{k}n}_j = 0 \tag{18}$$

produces renormalized energy bands $E_{\mathbf{k}n}$ and wave functions $\sum_j B^{\mathbf{k}n}_j |\mathbf{k}j\rangle$ of the quasiparticles.

D. Charge Density

In order to find a new density, we calculate a Gutzwiller density matrix operator in the LDA representation

$$\rho^{G\mathbf{k}}_{j'j} = \sum_{j''} f_{\mathbf{k}j''} \left(\sum_{\alpha} \sqrt{z_\alpha} \langle \mathbf{k}j'|\phi_\alpha\rangle\langle\phi_\alpha|\mathbf{k}''\rangle + \langle \mathbf{k}j'|\mathbf{k}j''\rangle - \sum_{\alpha} \langle \mathbf{k}j'|\phi_\alpha\rangle\langle\phi_\alpha|\mathbf{k}j''\rangle \right) \times \left(\sum_{\beta} \sqrt{z_\beta} \langle \mathbf{k}j''|\phi_\beta\rangle\langle\phi_\beta|\mathbf{k}j\rangle + \langle \mathbf{k}j''|\mathbf{k}j\rangle - \sum_{\beta} \langle \mathbf{k}j''|\phi_\beta\rangle\langle\phi_\beta|\mathbf{k}j\rangle \right) + \sum_{\alpha} \langle \mathbf{k}j'|\phi_\alpha\rangle(1-z_\alpha)\rho_\alpha\langle\phi_a|\mathbf{k}j\rangle \tag{19}$$

where

$$\rho_\alpha = \sum_{\mathbf{k}j} f_{\mathbf{k}j} \langle \mathbf{k}j|\phi_\alpha\rangle\langle\phi_\alpha|\mathbf{k}j\rangle \tag{20}$$

Diagonalizing it produces new occupation numbers $n_{\mathbf{k}\lambda}$

$$\sum_j (\rho^{G\mathbf{k}}_{j'j} - \delta_{j'j} n_{\mathbf{k}\lambda}) C^{\mathbf{k}\lambda}_j = 0 \tag{21}$$

so that the density of quasiparticles in real space is given by

$$\rho^G(\mathbf{r}) = \sum_{\mathbf{k}\lambda} n_{\mathbf{k}\lambda} \left(\sum_{j'} C^{\mathbf{k}\lambda}_{j'} |\mathbf{k}j'\rangle \right) \left(\sum_j C^{\mathbf{k}\lambda *}_j \langle \mathbf{k}j| \right) \tag{22}$$

E. Incompleteness of Basis

To see the importance of the issue, let us examine a shift of the LDA eigenstates $\epsilon_{\mathbf{k}j}$ by arbitrary value x. We obtain the new Gutzwiller Hamiltonian as the old one plus the correction

$$\langle \mathbf{k}j'|\tilde{H}^G|\mathbf{k}j\rangle = \langle \mathbf{k}j'|H^G|\mathbf{k}j\rangle + x o_{j'j}(\mathbf{k}) \tag{23}$$

where $o_{j'j}(\mathbf{k})$ is a matrix that can be proved to be equal to $\delta_{j'j}$ only under the assumption that the LDA wave functions form a mathematically complete basis set, i.e.

$$\sum_{j''} \langle \phi_\alpha|\mathbf{k}j''\rangle\langle \mathbf{k}j''|\phi_\beta\rangle = \delta_{\alpha\beta} \tag{24}$$

Unfortunately, modern electronic structure methods deal with finite basis sets, and the last relationship is only approximately satisfied. As a result, different choices of energy zero for the LDA eigenvalues $\epsilon_{\mathbf{k}j}$ may lead to slightly different output, although in our application to well–localized Cerium 4f electrons, this introduces only minor noise in our calculated results. In the following, we always assume that the LDA eigenvalues are measured with respect to the Fermi energy which is the only physically relevant energy in this problem.

F. Double Counting Potential

As one sees from Eq.(16) the actual self–energy correction used in the LDA+G calculation is $\Sigma_\alpha(0) - V_{DC,\alpha}$. Frequently, a so called LDA+U version[46] of double counting potential $V_{DC,\alpha}$ is used, that for our case is just an orbital–independent energy shift given by

$$V^{LDA+U}_{DC} = U(n_f - 1/2), \tag{25}$$

where n_f is the average number of f electrons which at Ce f–shell is close to unity. As one sees, this correction has just an overall level shift by $U/2$ and does not modify the Gutzwiller extracted spin–orbit and crystal fields encoded in the α dependence of $\Sigma_\alpha(0)$. Unfortunately, it is not exactly clear whether the overall level shift of Ce f electrons has a physical effect, since the standard LDA+U double counting was introduced in connection to the Hartree Fock value of the self–energy which is the value at infinite frequency, $\Sigma(\infty)$. It therefore may not be suited for correcting low energy physics of the heavy fermion systems.

As a result, in this work we adopt a different strategy in order to elucidate the physics of orbital selectivity in Ce heavy fermion compounds: our calculations are first performed without $\Sigma_a(0)$ correction assuming that the double counting potential

$$V^{(1)}_{DC,\alpha} = \Sigma_\alpha(0). \tag{26}$$

It has an important justification that the LDA calculated Fermi surfaces do not acquire any modifications as was the past evidence for some heavy fermion uranium compounds[47]. Second, we introduce the crystal field averaged double counting

$$V_{DC}^{(2)} = \frac{1}{N}\sum_{\alpha}^{N}\Sigma_{\alpha}(0) \tag{27}$$

which keeps the average position of the f–level intact but allows for its crystal field modifications found self–consistently via the LDA+G procedure. Since both $V_{DC,\alpha}^{(1)}$ and $V_{DC,\alpha}^{(2)}$ rely on Gutzwiller extracted $\Sigma_{\alpha}(0)$, which itself is obtained from the LDA+G functional minimization procedure, the entire method is still variational and allows an accurate estimate of the total energy. Comparing calculations with two types of double counting, important conclusions can be drawn on which exactly orbitals of a given heavy fermion system play a major role in its electronic mass enhancement.

III. RESULTS AND DISCUSSION

We are interested in calculating the mass enhancement parameters of Cerium f electrons which in a simple single band theory would be given by the ratio of m^*/m_{LDA}. A common approach to extract this data is to compare the values of the Sommerfeld coefficient γ evaluated using the LDA density of states at the Fermi level $N_{LDA}(0)$

$$\gamma_{LDA} = \frac{\pi^2}{3}k_B N_{LDA}(0) \tag{28}$$

with the measured electronic specific heat which, according to the Fermi liquid theory, behaves at low temperatures as γT. However, some care should be taken when adopting this procedure. First, densities of states of real systems include muliband features and contributions from both heavy and light electrons. Second, LDA densities of states assume some crystal field effects which should in general be supplemented by many body corrections encoded in $\Sigma_a(0)$. Therefore not only band narrowing but also level shifts are expected to occur in real life on top of LDA. Third, many of the materials discussed in our work undergo either antiferromagnetic or superconducting transition before reaching $T \to 0$ limit. We quote the data for $\gamma_{\rm exp}$ in Table I using the data for their lowest temperature paramagnetic phases.

There are several other ways to access this information that we are going to use in this work. Optical spectroscopy experiments can provide access to effective masses but those are frequency dependent. Angle–resolved photoemission spectroscopy (ARPES) experiments measure directly one–electron spectral functions

$$A(\mathbf{k},\omega) = \frac{|\Im\Sigma(\mathbf{k},\omega)|}{(\omega - \Re\Sigma(\mathbf{k},\omega))^2 + \Im\Sigma^2(\mathbf{k},\omega)} \tag{29}$$

Here $\Re\Sigma$ is the real part and $\Im\Sigma$ is the imaginary part of the electronic self–energy. Under the assumption of the locality of self–energy, the quasiparticle residues

$$z = \left(1 - \frac{\partial\Re\Sigma(\omega)}{\partial\omega}\right)^{-1} \tag{30}$$

can be extracted by comparing ARPES spectra against calculated LDA energy bands.

The dHvA effect is another powerful experimental technique which measures the properties of the Fermi surface properties under applied magnetic field[45]. LDA calculation can identify each cyclotron orbit seen by the dHvA experiment and find corresponding effective masses. However, complexity in shapes of 3D Fermi surfaces in real systems also makes this method not perfect.

It is remarkable that the LDA+G calculation returns the orbital dependent quasiparticle residues z_α directly. In Table I, we are quoting these mass enhancement data and *not* the ones obtained via our calculated LDA+G densities of states.

A. α-Ce and γ-Ce

We first discuss our calculations for Cerium metal which is famous for its iso–structural phase transition from its α to γ phase that is accompanied by 15% of its volume expansion, and has attracted great attention in the past[4,5,48–51] and current[43] literature. It is remarkable that our LDA+G calculation can correct most of the error in predicting the volume of the α phase for both types of the double countings that we explore in this work. Moreover, as Fig. 1 illustrates, it clearly shows a double well type of behavior of the energy vs volume (with smaller/larger minima corresponding to α/γ phases) when using the crystal field averaged double counting $V_{DC}^{(2)}$ and the Hubbard U's within the range between 3.5 and 5.5 eV. This is in accord with the previous previous LDA+DMFT studies for Cerium[49]. Similar behavior has been also found when studying $\alpha \to \delta$ transition in metallic Plutonium[52].

The specific heat measurement of α–Ce gives its Sommerfeld coefficient $\gamma \sim 13$ mJ/(mol·K^2).[3]. The optical spectroscopy experiment[53] estimates the effective mass to be $\sim 6m_e$ in α–Ce and to be $\sim 20m_e$ in γ–Ce, indicating the itinerant/localized features of the α/γ phases. However, the estimated optical effective masses are frequency dependent.

Fig. 2 shows the dependence of the quasiparticle residues as a function of the Hubbard U for volumes corresponding to α– and γ–Ce where the left/right plots represent our calculations with $V_{DC}^{(1)}/V_{DC}^{(2)}$ type of double countings. It is clear when crystal/spin–orbital corrections are not taken into account (left plot), the effective masses for various Cerium orbitals are very similar in values and are not very strongly enhanced even for large

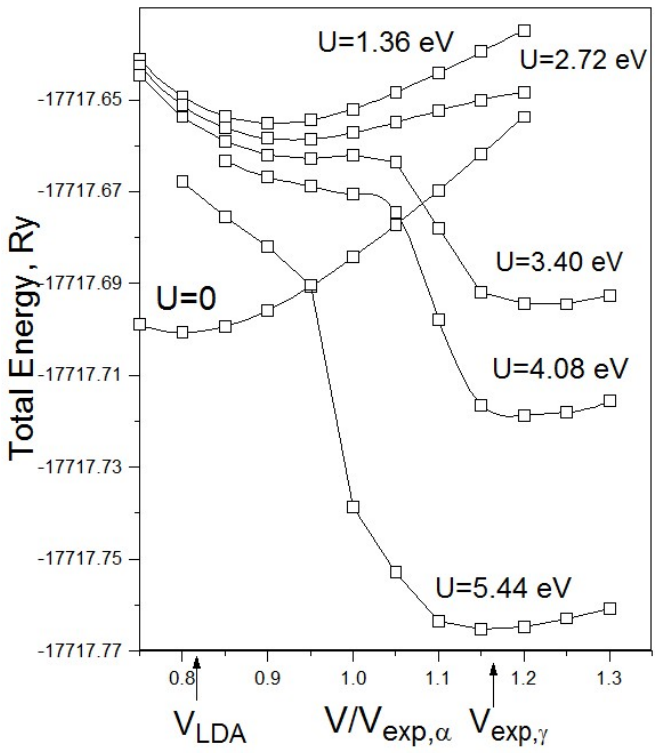

FIG. 1: (color online) Calculated total energy vs volume using the LDA+G method with several values of Hubbard U.

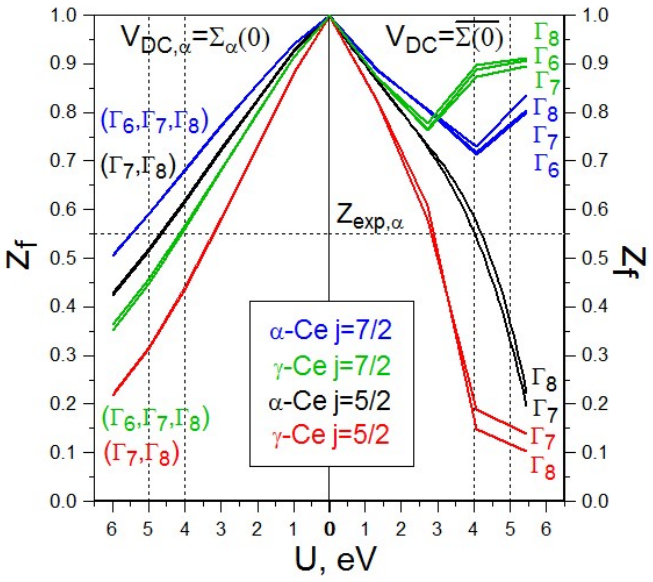

FIG. 2: (color online) Calculated dependence of quasiparticle residues as a function of Hubbard U in α and γ phases of Cerium metal using the LDA+G approach.

values of U. (We use relativistic cubic harmonics representation where $j = 5/2$ level is split onto Γ_7, Γ_8 and $j = 7/2$ onto $\Gamma_6, \Gamma_7, \Gamma_8$ states.) The situation changes dramatically when we account for the local self–energy correction (right plot): a Coulomb renormalized spin–orbit splitting pushes Γ_7, Γ_8 states of $j = 5/2$ manifold down and $\Gamma_6, \Gamma_7, \Gamma_8$ states of $j = 7/2$ manifold up. This results in redistributing the occupancies of the f–electrons which now reside mainly at $j = 5/2$ level. Thus, the effective degeneracy is 6 instead of 14 and the quasiparticle residues become much more sensitive to the values of U.

Actual comparison of the quasiparticle residues with experiment needs an accurate estimate of the Hubbard U for Cerium f–electrons which is typically around 5 eV, although, if the Hunds rule J˜1eV (important for the virtual f^2 state) is taken into account, the effective interaction is reduced a little bit to $U - J$. Due to a great sensitivity of quasiparticle residues to this parameter, and for the purposes of our work, we simply show in Table I the range of z's that one can obtain for the values of U in the range between 4 and 5 eV. For α–Ce we find them between 0.55 and 0.33 which are close to their experimental estimates. This is also consistent with the result of the LDA+DMFT calculation[54]. While there is no specific heat data for the γ phase, optical measurements[53] show a factor of 3–4 enhanced masses as compared to the ones of the α phase, and our reduced values of z's are in accord with this trend.

B. Ce-115s

We next discuss our applications to the so–called 115 series of Cerium heavy fermion compounds $CeMIn_5$ (M = Co, Rh, Ir). They have a tetragonal $HoCoGa_5$–type structure which results in additional splitting of all Γ_8 quadruplets into Γ_6 and Γ_7 doublets. Despite having similar structure and almost identical LDA electronic structures, these systems show very different properties which has attracted a great interest. $CeCoIn_5$ is a heavy fermion superconductor with critical temperature T_c = 2.3 K, highest known in Ce–based systems[6] and with the Sommerfeld coefficient $\gamma \cong 290$ mJ/(mol·K^2) measured just above T_c. $CeIrIn_5$ is also a superconductor with $T_c = 0.4$ K[8] with γ=720 mJ/(mol·K^2) above T_c that is nearly temperature independent. $CeRhIn_5$, on the other hand, is an antiferromagnet with Néel temperature T_N=3.8 K but becomes a superconductor with T_c= 2.1 K above a critical pressure $P_c \sim$16 kbar[7]. From the C/T data, there is a peak at T_N=3.8 K, indicating the onset of magnetic ordering. In order to find the electronic specific heat, one needs to use isostructural, nonmagnetic $LaRhIn_5$ to subtract the lattice contribution to C. However, it is difficult to define precisely the electronic specific heat above T_N due to the peaked structure. A simple entropy–balance construction gives a Sommerfeld coefficient $\gamma \geqslant 420$ mJ/(mol·K^2) for $T > T_N$.

Those different properties are considered as the result of the localized vs itinerant nature of the $4f$ electrons. The dHvA measurements for $CeCoIn_5$ have shown the effective cyclotron masses within the range from 9 to 20 m_0 which is consistent with the specific heat data[55,56]. The LDA calculation with a model of itinerant f electrons

shows a reasonable agreement with the dHvA data[57] while complete localization of the f electrons is needed to get the agreement with the angle–resolved photoemission spectroscopy(ARPES) data[58]. The dHvA experiment has been also performed for the antiferromagnetic state of $CeRhIn_5$[59,60]. Although earlier LDA calculation with the itinerant model shows some agreement with the experimental data[60], the localized nature of the f electrons was confirmed by the dHvA measurements in $Ce_xLa_{1-x}RhIn_5$[61] and by comparing the Fermi surfaces between $CeRhIn_5$ and $LaRhIn_5$[62]. With the application of pressure, the dramatic change of the Fermi surface was observed indicating the change from the localized antiferromagnetic state to the itinerant heavy fermion state[63]. For $CeIrIn_5$, there is some experimental controversy. The effective cyclone mass m_c^* is observed in the range from 6.3 to $45m_e$ indicating a large enhancement[64]. LDA with itinerant f electrons[57,64] explains well geometry and the volume of the Fermi surface but the band masses are much smaller of the cyclotron masses. The photoemission spectrum is well described by the LDA+DMFT calculation[27] where the degree of itineracy in $CeIrIn_5$ is though to be even larger than in $CeCoIn_5$[65]. Also, this method shows the calculated effective masses to be of the same order with the experimental one[66]. On the other hand, the ARPES study[67,68] shows that $CeIrIn_5$ and $CeRhIn_5$ have nearly localized $4f$ electrons.

The results of our paramagnetic LDA+G calculations for all three 115 compounds are presented in Table I. Similar to our calculation for Cerium, we find that the calculated effective masses are only moderately enhanced (z˜0.3−0.5) if we do not account for the crystal field/spin orbit corrections to the self–energy on top of the LDA. When we perform self–consistent calculation including the level shifts, much smaller values of the quasiparticle residues can be reached. Fig. 3 illustrates this behavior for $CeCoIn_5$. The situation here is similar to Cerium where the spin–orbit coupling gets renormalized by correlations making the effective degeneracy of the f–electrons equal 6. Actual values of the quasiparticle residues in Table I are given for U equal 4 and 5 eV: we see that the estimated z is the largest for $CeCoIn_5$ while the f electrons are more localized in $CeRhIn_5$ and $CeIrIn_5$. The residual discrepancies can be attributed to the above discussed uncertainties seen in experiments and also to the intrinsic error connected to the Gutzwiller procedure as our prior studies of the performance of this method against Quantum Monte Carlo approach have shown a 30% type of error[69].

C. Ce-122s

We finally discuss our applications to Ce 122 types of systems. By itself, RM_2X_2 is an enormous class of ternary intermetallic compounds with over hundreds of members, where R is a rare–earth element, M denotes a transition metal ($3d$. $4d$, or $5d$) and X is either silicon or

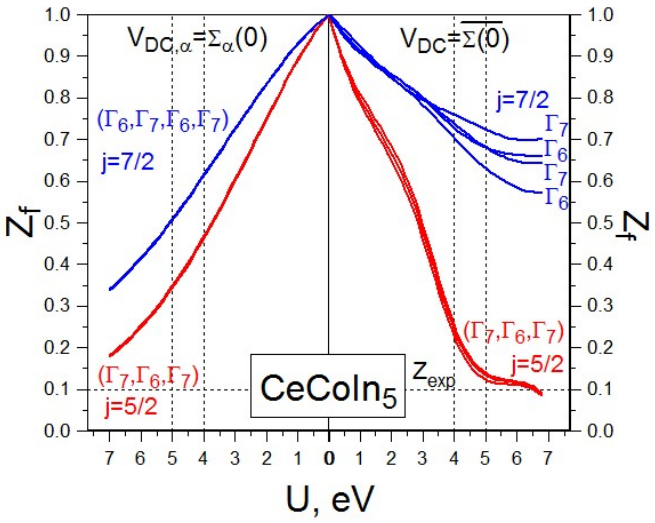

FIG. 3: (color online) Calculated dependence of quasiparticle residues as a function of Hubbard U in $CeCoIn_5$ using the LDA+G approach.

germanium. After its first discovery of superconductivity with a transition temperature $T_c \simeq 0.5$ K in $CeCu_2Si_2$[13], the interest in this family awakens, especially due to the interplay between antiferromagnetic and superconducting orders. Here we focus on the subclass CeM_2Si_2 (M = Mn, Fe, Co, Ni, Cu, Ru, Rh, Pd, Ag) where all members have body–centered tetragonal $ThCr_2Si_2$–type structure with space group $I4/mmm$.

For $M = 3d$ series, no magnetic order is found except for $CeMn_2Si_2$ where the Mn local moments order below 379 K[70]. For $CeCu_2Si_2$, the electronic specific heat coefficient $\gamma \simeq 1000$ mJ/(mol·K^2) is the largest one among this family. On the other hand, $CeFe_2Si_2$, $CeCo_2Si_2$ and $CeNi_2Si_2$ are weak paramagnets with relatively small values of γ value which is shown in Table I. These three compounds are also known as valence fluctuation systems.

For $M = 4d$ series, first, $CeRu_2Si_2$ is known as a archetypal Kondo lattice compound: it is a paramagnet with a relative large $\gamma \simeq 350$ mJ/(mol·K^2). The other three are antiferromagnets at low temperatures: $CeRh_2Si_2$ has the highest ordering temperature 36–39 K[71,72] while $CePd_2Si_2$[21,71] and $CeAg_2Si_2$[71,73] order antiferromagnetically at 8.5-10 K an 8-10 K, respectively. With the application of pressure, superconductivity was found in $CeRh_2Si_2$[74] and in $CePd_2Si_2$[75]. $CeRu_2Si_2$ is unique in this subclass since the superconductivity is not observed down to a few mK. This makes it best target material for studying its heavy fermion state. Interestingly, here a metamagnetic transition was found and extensively studied[76]. The cyclotron effective mass $m_c \sim 120m_e$ is observed in the dHvA experiment indicating the renormalized heavy fermion state[77]. The electronic structure calculation using LDA with itinerant f–electron model qualitatively explains the dHvA data[78–80] The metamagnetic transition was also stud-

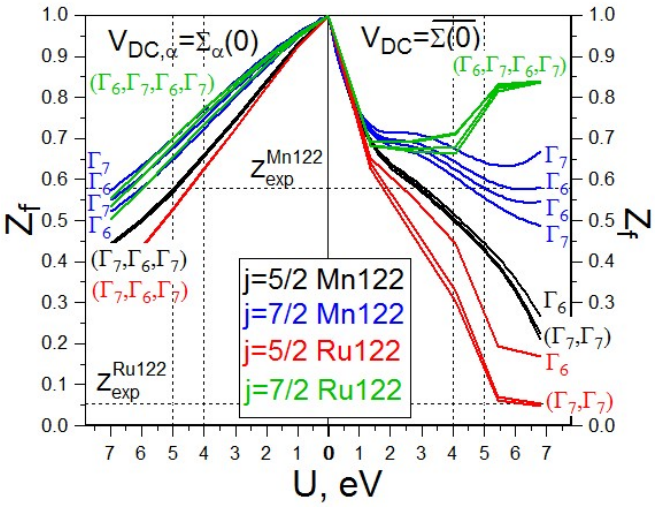

FIG. 4: (color online) Calculated dependence of quasiparticle residues as a function of Hubbard U in $CeMn_2Si_2$ and $CeRu_2Si_2$ using the LDA+G approach.

ied by dHvA experiments[81–83] demonstrating that the f–electron character is changed from itinerant to localized across the metamagnetic transition. All members of this family of compounds were put into the Doniach (T_N vs J_K) phase diagram[84]. Later, using the LDA+DMFT scheme, the phase diagram was renewed[28].

Results of our applications to Ce 122s are presented in Table 1. They assume a paramagnetic heavy fermion state for all systems and the experimental $\gamma's$ are extracted from the specific heat data measured above the temperatures of antiferromagnetic/superconducting transition. For the 122 systems with 3d elements such as Mn,Fe,Co,Ni, the LDA+G procedure returns only moderately enhanced electron masses which we find in agreement with the experiment. An example of the dependence of z_α vs U is shown on Fig. 4 for Mn based 122, where the Coulomb renormalizing spin–orbit splitting is essential to reduce the orbital degeneracy from 14 to 6 when using the crystal field averaged double counting, $V_{DC}^{(2)}$. This is similar to our findings in Ce and Ce–115 systems. Our calculation for Cu based 122 shows that its quasiparticle residues are very sensitive to the values of U above 4 eV. In fact, it is beginning to reach almost zero values when U approaches 5 eV. It is also known experimentally that this system shows enormous mass enhancement just before it goes into superconducting state.

The 122 compounds with 4d elements (Ru, Rh, Pd, Ag) exhibit strongly renormalized quasiparticle masses. Our LDA+G calculations listed in Table I correctly follow this trend where we see a strong reduction of z's as compared to our calculations with 3d elements. We also find another interesting effect: with increasing U the effective degeneracy of the f electrons acquires a reduction not only due to the Coulomb assisted renormalization of spin–orbit splitting but also renormalization of the crystal fields: Fig. 4 shows this behavior for Ru-122 where we see that the values of z become different for various crystal field levels of the $j = 5/2$ manifold: one Γ_6 and two Γ_7 doublets. We find that a similar effect occurs in all other 4d types of Ce 122s and the last column of Table I lists our results showing which particular orbitals exhibit the strongest mass enhancement.

IV. CONCLUSION

In conclusion, using a recently proposed LDA+G approach we have studied quasiparticle mass renormalizations in several classes of Ce heavy fermion compounds. We find that the calculation gives correct trends across various systems as compared to the measured Sommerfeld coefficient and reproduces the order of magnitude of the experimental value. We also uncover an interesting orbital dependency of the quasiparticle residues for each studied compound which provides an important physical insight on how correlations affect the effective degeneracy of Cerium f–electrons placed in various crystallographic environments.

Acknowledgements

The authors are grateful to Y.–F. Yang for useful comments. This work was supported by US DOE Nuclear Energy University Program under Contract No. 00088708.

[1] For a review, see, e.g., A. C. Hewson, *The Kondo Problem to Heavy Fermions* (Cambridge University Press, Cambridge, 1997).
[2] For a review, see, e.g., Theory of Inhomogeneous Electron Gas, ed.by S. Lundqvist and N. H. March (Plenm, New York, 1983).
[3] N. T. Panousis, K. A. Gschneidner Jr.,Solid State Commun. **8**, 1779 (1970).
[4] B. Johansson, Philos. Magn. **30**, 469 (1974).
[5] J. W. Allen, R. M. Martin, Phys. Rev. Lett. **49**, 1106 (1982).
[6] C. Petrovic, P. G. Pagliuso, M. F. Hundley, R. Movshovich, J. L. Sarrao, J. D. Thompson, Z. Fisk, and P. Monthoux, J. Phys.: Condens. Matter **13**, L337 (2001).
[7] H. Hegger, C. Petrovic, E. G. Moshopoulou, M. F. Hundley, J. L. Sarrao, Z. Fisk, and J. D. Thompson, Phys. Rev. Lett. **84**, 4986 (2000).
[8] C. Petrovic, R. Movshovich, M. Jaime, P. G. Pagliuso, M. F. Hundley, J. L. Sarrao, Z. Fisk, and J. D. Thompson, Eur. Phys. Lett. **53**, 354. (2001).
[9] G. Liang, I. Perez, D. DiMarzio, M. Croft, D. C. Johnston, N. Anbalagan and T. Mihalisin, Phys. Rev. B **37**, 5970

(1988).
[10] M. Mihalik, M. Mihalik, and V. Sechovský, Physica B **359–361**, 163 (2005).
[11] G. Nakamoto, A. Fuse, M. Kurisu, and T. Shigeoka, J. Magn. Magn. Mater. **272-276**, e75 (2004).
[12] J. J. Lu, M. K. Lee, Y. M. Lu, J. F. Chou, L.Y. Jang, Solid State Commun. **135**, 505 (2005).
[13] F. Steglich, J. Aarts, C. D. Bredl, W. Lieke, D. Meschede, W. Franz, and H. Schäfer, Phys. Rev. Lett. **43**, 1892 (1979).
[14] M. Hunt, P. Meeson, P.-A. Probst, P. Reinders, M. Springford, W. Assmus and W. Sun. J. Phys.: Condens. Matter **2**, 6859 (1990).
[15] H. Harima and A. Yanase, J. Phys. Soc. Jpn. **60**, 21 (1991).
[16] F. Steglich, U. Rauchschwalbe, U. Gottwick, H. M. Mayer, G. Sparn, N. Grewe, U. Poppe, and J. J. M. Franse, J. Appl. Phys. **57**, 3054 (1985).
[17] J. D. Thompson, J. O. Willis, C. Godart, D. E. MacLaughlin, and L. C. Gupta, Solid State Commun. **56**, 169 (1985).
[18] M. J. Besnus, J. P. Kappler, P. Lehmann, and A. Meyer, Solid State Commun. **55**, 779 (1985).
[19] T. Graf, J. D. Thompson, M. F. Hundley, R. Movshovich, Z. Fisk, D. Mandrus, R. A. Fisher, and N. E. Phillips, Phys. Rev. Lett. **78**, 3769 (1997).
[20] S. K. Dhar, E. V. Sampathkumaran, Phys. Lett. A **121**, 454 (1987).
[21] R. A. Steeman, E. Frikkee, R. B. Helmholdt, A. A. Menovsky, J. Van den Berg, G. J Nieuwenhuys, and J. A. Mydosh, Solid State Commun. **66**, 103 (1988).
[22] X. Y. Deng, X. Dai, and Z. Fang, Eur. Phys. Lett. **83**, 3008 (2008).
[23] K. M. Ho, J. Schmalian, and C. Z. Wang, Phys. Rev. B **77**, 073101 (2008).
[24] X. Y. Deng, L. Wang, X. Dai, and Z. Fang, Phys. Rev. B **79**, 075114 (2009);
[25] Y. X. Yao, C. Z. Wang, and K. M. Ho, Phys. Rev. B **83**, 245139 (2011).
[26] For a review, see, e.g., G. Kotliar, S. Y. Savrasov, K. Haule, V. S. Oudovenko, O. Parcollet, and C. A. Marianetti, Rev. Mod. Phys. **78**, 865 (2006).
[27] J. H. Shim, K. Haule, and G. Kotliar, Science **318**, 1615 (2007).
[28] M. Matsumoto, M. J. Han, J. Otsuki, S. Y. Savrasov, Phys. Rev Lett. **103**, 096403 (2009).
[29] P. Werner, A. Comanac, L. de' Medici, M. Troyer, and A. J. Millis, Phys. Rev. Lett. **97**, 076405 (2006).
[30] J. Otsuki, H. Kusunose, P. Werner, and Y. Kuramoto, J. Phys. Soc. Jpn. **76**, 114707 (2007).
[31] M. C. Gutzwiller, Phys. Rev. Lett. **10**, 159 (1963); Phys. Rev. **134**, A923 (1964); **137**, A1726 (1965).
[32] J. Bünemann, F. Gebhard, and W. Weber, J. Phys.: Condens. Matter **9**, 7343 (1997).
[33] J. Bünemann, W. Weber, and F. Gebhard, Phys. Rev. B **57**, 6896 (1998).
[34] W. Metzner and D. Vollhardt, Phys. Rev. Lett. **62**, 324 (1989).
[35] W. Metzner, Z. Phys. B: Condens. Matter **77**, 253 (1989).
[36] G. Kotliar and A. E. Ruckenstein, Phys. Rev. Lett. **57**, 1362 (1986).
[37] F. Gebhard, Phys. Rev. B **44**, 992 (1991).
[38] F. Lechermann, A. Georges, G. Kotliar, and O. Parcollet, Phys. Rev. B **76**, 155102 (2007).
[39] J. Bünemann and F. Gebhard, Phys. Rev. B **76**, 193104 (2007).
[40] G.-T. Wang, X. Dai, and Z. Fang, Phys. Rev. Lett. 101, 066403 (2008).
[41] G.T. Wang, Y. Qian, G. Xu, X. Dai, and Z. Fang, Phys. Rev. Lett. 104, 047002 (2010).
[42] M.-F. Tian, X.Y. Deng, Z. Fang, and X. Dai, Phys. Rev. B 84, 205124 (2011).
[43] N. Lanatà, Y.–X. Yao, C.-Z. Wang, K.–M. Ho, J. Schmalian, K. Haule, G. Kotliar, Phys. Rev. Lett. **111**, 196801 (2013).
[44] S. Y. Savrasov, Phys. Rev. B **54**, 16470 (1996).
[45] Y. Onuki and R. Settai, Low Temp. Phys. **38**, 89 (2012).
[46] For a review, see, e.g., V. I. Anisimov, F. Aryasetiawan, and A. I. Lichtenstein, J. Phys.: Condens. Matter **9**, 767 (1997).
[47] C. S. Wang, M. R. Norman, R. C. Albers and A. M. Boring, W. E. Pickett, H. Krakauer, N. E. Christensen, Phys. Rev. B 35, 7260 (1987).
[48] M. B. Zölfl, I. A. Nekrasov, Th. Pruschke, V. I. Anisimov and J. Keller, Phys. Rev. Lett. **87**, 276403 (2001).
[49] K. Held, A. K. McMahan and R. T. Scalettar, Phys. Rev. Lett. **87**, 276404 (2001).
[50] K. Haule, V. Oudovenko, S. Y. Savrasov, and G. Kotliar, Phys. Rev. Lett. **94**, 036401 (2005).
[51] B. Amadon, S. Biermann, A. Georges, and F. Aryasetiawan, Phys. Rev. Lett. **96**, 066402 (2006).
[52] S. Y. Savrasov, G. Kotliar, E. Abrahams, Nature 410, 793 (2001).
[53] J. W. van der Eb, A. B. KuzÕmenko, and D. van der Marel, Phys. Rev. Lett. **86**, 3407 (2001).
[54] O. Sakai, Y. Shimizu and Y. Kaneta, J. Phys. Soc. Jpn. **74**, 2517 (2005).
[55] D. Hall, E. C. Palm, T. P. Murphy, S. W. Tozer, Z. Fisk, U. Alver, R. G. Goodrich, J. L. Sarrao, P. G. Pagliuso, and T. Ebihara, Phys. Rev. B **64**, 212508 (2001).
[56] R. Settai, H. Shishido, S. Ikeda, Y. Murakawa, M. Nakashima, D. Aoki, Y. Haga, H. Harima, and Y. Ōnuki, J. Phys.: Condens. Matter **13**, L627 (2001).
[57] S. Elgazzar, I. Opahle, R. Hayn, and P. M. Oppeneer, Phys. Rev. B **69**, 214510 (2004).
[58] A. Koitzsch, I. Opahle, S. Elgazzar, S. V. Borisenko, J. Geck, V. B. Zabolotnyy, D. Inosov, H. Shiozawa, M. Richter, M. Knupfer, J. Fink, B. BÃ$\frac{1}{4}$chner, E. D. Bauer, J. L. Sarrao, and R. Follath, Phys. Rev. B **79**, 075104 (2009).
[59] A. L. Cornelius, A. J. Arko, J. L. Sarrao, and N. Harrison, Phys. Rev. B **62**, 14181 (2000).
[60] D. Hall, E. C. Palm, T. P. Murphy, S. W. Tozer, C. Petrovic, E. Miller-Ricci, L. Peabody, C. Q. H. Li, U. Alver, R. G. Goodrich, J. L. Sarrao, P. G. Pagliuso, J. M. Wills, and Z. Fisk, Phys. Rev. B **64**, 064506 (2001).
[61] U. Alver, R. G. Goodrich, N. Harrison, D. W. Hall, E. C. Palm, T. P. Murphy, S. W. Tozer, P. G. Pagliuso, N. O. Moreno, J. L. Sarrao, and Z. Fisk, Phys. Rev. B **64**, 180402 (R) (2001).
[62] H. Shishido, R. Settai, D. Aoki, S. Ikeda, H. Nakawaki, N. Nakamura, T. Iizuka, Y. Inada, K. Sugiyama, T. Takeuchi, K. Kindo, T. C. Kobayashi, Y. Haga, H. Harima, Y. Aoki, T. Namiki, H. Sato, and Y. Ōnuki, J. Phys. Soc. Jpn. **71**, 162 (2002).
[63] H. Shishido, R. Settai, H. Harima and Y. Ōnuki, J. Phys. Soc. Jpn. **74**, 1103 (2005).
[64] Y. Haga, Y. Inada, H. Harima, K. Oikawa, M. Murakawa, H. Nakawaki, Y. Tokiwa, D. Aoki, H. Shishido, S. Ikeda,

N. Watanabe, and Y. Ōnuki, Phys. Rev. B **63**, 060503(R) (2001).
[65] K. Haule, C. -H. Yee, and K. Kim, Phys. Rev. B **81**, 195107 (2010).
[66] H. C. Choi, B. I. Min, J. H. Shim, K. Haule, and G. Kotliar, Phys. Rev. Lett. **108**, 016402 (2012)
[67] S. I. Fujimori, T. Okane, J. Okamoto, K. Mamiya, Y. Muramatsu, A. Fujimori, H. Harima, D. Aoki, S. Ikeda, H. Shishido, Y. Tokiwa, Y. Haga, and Y. Ōnuki, Phys. Rev. B **67**, 144507 (2003).
[68] S. I. Fujimori, A. Fujimori, K. Shimada, T. Narimura, K. Kobayashi, H. Namatame, M. Taniguchi, H. Harima, H. Shishido, S. Ikeda, D. Aoki, Y. Tokiwa, Y. Haga, and Y. Ōnuki, Phys. Rev. B **73**, 224517 (2006).
[69] S. Y. Savrasov, K. Haule, V. Oudovenko, D. Villani, G. Kotliar, Phys. Rev. B **71**, 115117 (2005).
[70] A. Szytula and I. Szott, Solid State Commun. **40**, 199 (1981).
[71] B. H. Grier, J. M. Lawrence, V. Murgai and R. D. Parks, Phys. Rev. B **29**, 2664 (1984).
[72] S. Quezel, J. Rossat-Mignod, B. Chevalier, P. Lejay and J. Etourneau, Solid State Commun. **49**, 685 (1984)
[73] T. T. M. Palstra, A. A. Menovsky, G. J. Nieuwenhuys and J. A. Mydosh, J. Magn. Magn. Mater. **54-57**, 435 (1986).
[74] R. Movshovich, T. Graf, D. Mandrus, J. D. Thompson, J. L. Smith, and Z. Fisk, Phys. Rev. B **53**, 8241 (1996).
[75] N. D. Mathur, F. M. Grosche, S. R. Julian, I. R. Walker, D. M. Freye, R. K. W. Haselwimmer, and G. G. Lonzarich, Nature (London) **394**, 39 (1998).
[76] P. Haen, J. Flouquet, F. Lapierre, P. Lejay, and G. Remenyi, J. Low Temp. Phys. **67**, 391 (1987).
[77] H. Aoki, S. Uji, A. K. Albessard, and Y. Ōnuki, J. Phys. Soc. Jpn. **61**, 3457 (1992).
[78] H. Yamagami and A. Hasegawa, J. Phys. Soc. Jpn. **61**, 2388 (1992).
[79] H. Yamagami and A. Hasegawa, J. Phys. Soc. Jpn. **62**, 592 (1993).
[80] E. K. R. Runge, R. C. Albers, N. E. Christensen, and G. E. Zwicknagl, Phys. Rev. B **51**, 10375 (1995).
[81] Y. Ōnuki, I. Umehara, A. K. Albessard, T. Ebihara, and K. Satoh, J. Phys. Soc. Jpn. **61**, 960 (1992).
[82] H. Aoki, S. Uji, A. K. Albessard, and Y. Ōnuki, J. Phys. Soc. Jpn. **62**, 3157 (1993).
[83] H. Aoki, S. Uji, A. K. Albessard, and Y. Ōnuki, Phys. Rev. Lett. **71**, 2110 (1993).
[84] T. Endstra, G. J. Nieuwenhuys, and J. A. Mydosh, Phys. Rev. B **48**, 9595 (1993).